

# Dalton Transactions

Accepted Manuscript



This is an *Accepted Manuscript*, which has been through the Royal Society of Chemistry peer review process and has been accepted for publication.

*Accepted Manuscripts* are published online shortly after acceptance, before technical editing, formatting and proof reading. Using this free service, authors can make their results available to the community, in citable form, before we publish the edited article. We will replace this *Accepted Manuscript* with the edited and formatted *Advance Article* as soon as it is available.

You can find more information about *Accepted Manuscripts* in the [Information for Authors](#).

Please note that technical editing may introduce minor changes to the text and/or graphics, which may alter content. The journal's standard [Terms & Conditions](#) and the [Ethical guidelines](#) still apply. In no event shall the Royal Society of Chemistry be held responsible for any errors or omissions in this *Accepted Manuscript* or any consequences arising from the use of any information it contains.

Cite this: DOI: 10.1039/c0xx00000x

www.rsc.org/xxxxxx

ARTICLE TYPE

# Assembly and photocatalysis of two novel 3D Anderson-type polyoxometalate-based metal-organic frameworks constructed from isomeric bis(pyridylformyl)piperazine ligands

Xiuli Wang,<sup>\*a</sup> Zhihan Chang, Hongyan Lin, Aixiang Tian, Guocheng Liu, Juwen Zhang

<sup>5</sup> Received (in XXX, XXX) Xth XXXXXXXXXX 20XX, Accepted Xth XXXXXXXXXX 20XX

DOI: 10.1039/b000000x

Two novel Anderson-type polyoxometalates (POMs)-based metal-organic frameworks (MOFs), namely,  $H\{Cu_2(\mu_2-OH)_2L^1[CrMo_6(OH)_6O_{18}]\} \cdot 4H_2O$  (**1**),  $\{Cu_2L^2[CrMo^VI_5Mo^V(OH)_6O_{18}](H_2O)_4\} \cdot 4H_2O$  (**2**) ( $L^1 = N, N'$ -bis(3-pyridinecarboxamide)-piperazine,  $L^2 = N, N'$ -bis(4-pyridinecarboxamide)-piperazine), are hydrothermally synthesized and structurally characterized by single-crystal X-ray diffraction, IR spectra, powder X-ray diffraction (PXRD) and thermogravimetric analyses (TGA). In complex **1**, the hexadentate  $[CrMo_6(OH)_6O_{18}]^{3-}$  polyoxoanion bridges the  $Cu^{II}$  ions to generate a 2D Cu-POM inorganic layer, which is further extended by the  $\mu_2$ -bridging  $L^1$  ligands (via ligation of pyridyl nitrogen atoms) to form a 3D MOF with 4,6-connected  $\{4^4 \cdot 6^{10} \cdot 8\}\{4^4 \cdot 6^2\}$  topology. Complex **2** is also a 3D POM-based MOF exhibiting a  $\{4^2 \cdot 8^4\}$  topology, which is constructed from the quadridentate  $[CrMo^VI_5Mo^V(OH)_6O_{18}]^{4-}$  polyoxoanions and  $\mu_4$ -bridging  $L^2$  ligands (via ligation of pyridyl nitrogen and carbonyl oxygen atoms). The different coordination modes of POM polyanions and the isomeric bis(pyridylformyl)piperazine ligands play key roles in the construction of the title complexes. In addition, the photocatalytic activities of the title complexes on the degradation of methylene blue (MB) under UV, visible light and sunlight irradiation have been investigated in detail.

## Introduction

Polyoxometalates (POMs), as a versatile family of molecular metal-oxygen clusters, exhibit diverse structures and tunable properties, which have been found numerous applications in catalysis, analytical chemistry, material science, magnetism and medicine.<sup>1</sup> Recently, a significant branch in POM chemistry field is the design and synthesis of POMs-based hybrid frameworks with important and potential applications, in which POMs are usually employed as inorganic building blocks or templates.<sup>2</sup> Many factors such as initial reactants and their stoichiometry ratios, nature of organic ligands and metal ions, pH value and temperature, can influence the ultimate architectures of POMs-based complexes.<sup>3</sup> Of all these factors, the selection of organic ligands is extremely important in the self-assembly process of prospective POMs-based MOFs, because organic ligands may control and adjust the topologies of final MOFs. For example, Ma's group have reported a series of  $Mo_8O_{26}^{4-}$ -based metal-organic complexes, in which the coordination modes of the

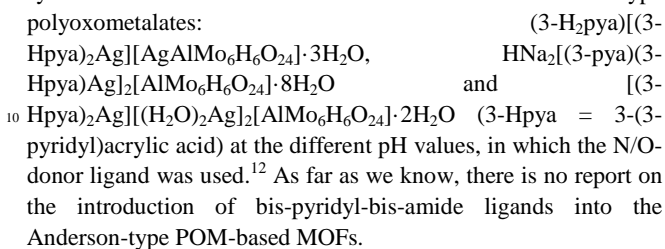
isomeric organic ligands have a great effect on the final structures.<sup>4</sup> Our group also reported several Keggin-type POM-based metal organic complexes constructed from the flexible ligands with different space lengths, which influence the formation and structures of the target complexes.<sup>5</sup>

Anderson-type polyoxoanion consists of a metal-oxygen octahedron at the center surrounded by six  $MoO_6$  (or  $WO_6$ ) octahedra. Compared to classical Keggin or Dawson-type POMs, the Anderson-type polyoxoanion exhibits attractive planar structure, and each Mo (or W) atom has two terminal O atoms, which make them possess high reactivity and conduce to coordinate with the transition metal ions.<sup>6</sup> In addition, Anderson-type polyoxoanions with rich O coordination sites show different coordination modes, which may result in various and novel structures.<sup>7</sup> Currently, lots of neutral N-donor ligands including pyridine-, imidazole-, triazole-, and tetrazole-based ligands have been introduced into the POM-based complexes family.<sup>8</sup> However, the reports on the combination between Anderson-type POMs and metal-organic motifs based on N-donor and N/O-donor ligands are relatively limited, especially those high dimensional architectures.<sup>9</sup> Das's group have reported two Anderson-type heteropolyanion-supported copper phenanthroline complexes,  $[Al(OH)_6Mo_6O_{18}\{Cu(phen)(H_2O)_2\}_2]^{1+}$  and  $[Al(OH)_6Mo_6O_{18}\{Cu(phen)(H_2O)Cl\}_2]^{1-}$ , in which

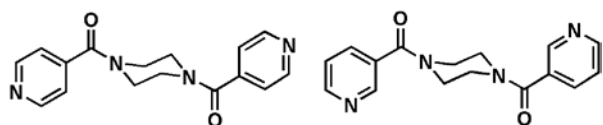
*Department of Chemistry, Bohai University, Jinzhou, 121000, P. R. China. Fax: +86-416-3400158; Tel: +86-416-3400158; Email: wangxiuli@bhu.edu.cn*

<sup>†</sup>Electronic Supplementary Information (ESI) available: IR Spectra, TG, and additional figures. CCDC 969174 and 969175. For ESI and crystallographic data in CIF or other electronic format see DOI: 10.1039/b000000x

phenanthrolines act as terminal ligands.<sup>10</sup> Wang's group also reported a series of new polyoxoanion-based inorganic-organic hybrids:  $(\text{C}_6\text{NO}_2\text{H}_5)[(\text{H}_2\text{O})_4(\text{C}_6\text{NO}_2\text{H}_5)\text{Ln}(\text{CrMo}_6\text{H}_6\text{O}_{24})]\cdot 4\text{H}_2\text{O}$  (Ln = Ce, Pr, La and Nd) with a chiral layer structure constructed from pyridine-4-carboxylic acid.<sup>11</sup> Besides, An's group synthesized three new architectures based on Anderson-type polyoxometalates:



Taking these into account, we are currently trying to introduce two isomeric semi-rigid bis(pyridylformyl)piperazine ligands N,N'-bis(3-pyridinecarboxamide)-piperazine ( $L^1$ ) and N,N'-bis(4-pyridinecarboxamide)-piperazine ( $L^2$ ) (Scheme 1) with different  $N_{\text{py}}$  substitution patterns to construct Anderson-type POM-based MOFs based on the following considerations: (a) As neutral nitrogen-/oxygen-donor ligands, both the pyridine moieties and the carbonyl groups of these ligands can coordinate with metal ions; (b) The conformational changes of the piperazine groups from the two ligands can meet the requirements of the coordination geometries of metal ions, which conduce to construct new complexes more easily; (c) The semi-rigid multidentate bridging ligands tend to construct the high-dimensional MOFs; (d) They not only possess similar composition, but also are positional isomers, which may generate different but often related frameworks. Fortunately, we successfully isolated two novel 3D Anderson-type POM-based MOFs,  $\text{H}\{\text{Cu}_2(\mu_2\text{-OH})_2\text{L}^1[\text{CrMo}_6(\text{OH})_6\text{O}_{18}]\}\cdot 4\text{H}_2\text{O}$  (**1**),  $\{\text{Cu}_2\text{L}^2[\text{CrMo}^{\text{VI}}\text{Mo}^{\text{V}}(\text{OH})_6\text{O}_{18}](\text{H}_2\text{O})_4\}\cdot 4\text{H}_2\text{O}$  (**2**) under the hydrothermal conditions. Complexes **1** and **2** represent the first examples of high-dimensional Anderson-type POM-based MOFs constructed from bis-pyridyl-bis-amide ligands. The excellent photocatalytic properties of the title complexes towards MB under UV, visible light and sunlight irradiation are investigated in this paper.



Scheme 1. The ligands used in this paper.

## Experimental

### Materials and characterization

All reagents and solvents for syntheses were purchased from commercial sources and used as received without further purification. The N/O-donor ligands  $L^1$  and  $L^2$  and  $\text{Na}_3[\text{CrMo}_6\text{H}_6\text{O}_{24}]\cdot 8\text{H}_2\text{O}$  were prepared according to the reported procedure.<sup>13</sup> FT-IR spectra (KBr pellets) were taken on a Scimitar 2000 Near FT-IR Spectrometer. Thermogravimetric analyses (TGA) were performed on a PyrisDiamond TG instrument under a flowing  $\text{N}_2$  atmosphere with a heating rate of  $10\text{ }^\circ\text{C}\cdot\text{min}^{-1}$ . Powder X-ray diffraction (PXRD) patterns were measured on an

Ultima IV with D/teX Ultra diffractometer at 40 kV, 40 mA with Cu  $K\alpha$  ( $\lambda = 1.5406\text{ \AA}$ ) radiation. UV-Vis absorption spectra were obtained using a SP-1901 UV-Vis spectrophotometer.

### Synthesis of $\text{H}\{\text{Cu}_2(\mu_2\text{-OH})_2\text{L}^1[\text{CrMo}_6(\text{OH})_6\text{O}_{18}]\}\cdot 4\text{H}_2\text{O}$ (**1**)

A mixture of  $\text{CuCl}_2\cdot 2\text{H}_2\text{O}$  (0.50 mmol),  $L^1$  (0.10 mmol)  $\text{Na}_3[\text{CrMo}_6\text{H}_6\text{O}_{24}]\cdot 8\text{H}_2\text{O}$  (0.24 mmol), and  $\text{H}_2\text{O}$  (10 mL) was stirred for 30 min at the room temperature. The pH value was then adjusted to about 4.0 using 1.0 M HCl. The suspension was transferred to a Teflon lined autoclave (25 mL) and kept at  $120\text{ }^\circ\text{C}$  for 4 days. After slowly cooled to room temperature, dark green block crystals of complex **1** were isolated from some green precipitate and solution, washed with distilled water, and dried in a desiccator at room temperature to give a yield of 32% based on Mo. IR (KBr pellet,  $\text{cm}^{-1}$ ): 3400 (s), 1614 (s), 1450 (m), 1275 (m), 947 (w), 901 (s), 824 (w), 644 (s), 579 (w).

### Synthesis of $\{\text{Cu}_2\text{L}^2[\text{CrMo}^{\text{VI}}\text{Mo}^{\text{V}}(\text{OH})_6\text{O}_{18}](\text{H}_2\text{O})_4\}\cdot 4\text{H}_2\text{O}$ (**2**)

A mixture of  $\text{CuSO}_4\cdot 2\text{H}_2\text{O}$  (0.42 mmol),  $L^2$  (0.10 mmol)  $\text{Na}_3[\text{CrMo}_6\text{H}_6\text{O}_{24}]\cdot 8\text{H}_2\text{O}$  (0.24 mmol), and  $\text{H}_2\text{O}$  (10 mL) was stirred for 30 min at the room temperature. The pH value was then adjusted to about 4.5 using 1.0 M HCl. After transferred to a Teflon lined autoclave (25 mL) and kept at  $120\text{ }^\circ\text{C}$  for 4 days, dark green block crystals of complex **2** were isolated from some dark green precipitate and solution, washed with distilled water, and dried in a desiccator at room temperature to give a yield of 22% based on Mo. IR(KBr pellet,  $\text{cm}^{-1}$ ): 3228 (s), 1614 (s), 1509 (w), 1471 (m) 1289 (m), 1166 (w), 936 (s), 885 (s), 646 (s).

Table 1 Crystal data and structure refinement for complexes **1-2**

Complex	<b>1</b>	<b>2</b>
Empirical formula	$\text{C}_{16}\text{H}_{33}\text{CrCu}_2\text{Mo}_6\text{N}_4\text{O}_{32}$	$\text{C}_{16}\text{H}_{38}\text{CrCu}_2\text{Mo}_6\text{N}_4\text{O}_{34}$
Formula weight	1548.18	1585.22
Crystal system	Triclinic	Triclinic
Space group	$P-1$	$P-1$
$a$ ( $\text{\AA}$ )	7.299(2)	7.6170(6)
$b$ ( $\text{\AA}$ )	11.469(4)	10.4420(8)
$c$ ( $\text{\AA}$ )	11.601(4)	13.8790(11)
$\alpha$ ( $^\circ$ )	103.137(4)	75.7970(10)
$\beta$ ( $^\circ$ )	99.656(5)	82.0180(10)
$\gamma$ ( $^\circ$ )	102.478(5)	71.7240(10)
$V$ ( $\text{\AA}^3$ )	899.1(5)	1013.86(14)
$Z$	1	1
$D_c$ ( $\text{g cm}^{-3}$ )	2.859	2.596
$\mu$ ( $\text{mm}^{-1}$ )	3.589	3.189
$F(000)$	747	768
Reflection collected	4503	5132
Unique reflections	3147	3528
parameters	277	286
$R_{\text{int}}$	0.0322	0.094
GO F	1.058	1.048
$R_1^a$ [ $I > 2\sigma(I)$ ]	0.0633	0.0238
$wR_2^b$ (all data)	0.1790	0.0630

$$^a R_1 = \frac{\sum ||F_o| - |F_c||}{\sum |F_o|}, \quad ^b wR_2 = \frac{\sum [w(F_o^2 - F_c^2)^2]}{\sum [w(F_o^2)^2]}^{1/2}$$

### X-Ray crystallographic study

Crystallographic data for the title complexes were collected on a Bruker Smart APEX II diffractometer with  $K\alpha$  ( $\lambda = 0.71069\text{ \AA}$ ) by  $\theta$  and  $\omega$  scan mode at 296 K. All the structures were solved by direct methods using the SHELXS program of the SHELXTL package and refined by full-matrix least-squares methods with SHELXL.<sup>14</sup> The H atoms on the C atoms were fixed in calculated

positions. However, the added H protons, the H atoms of the –OH groups and water molecules are not located in their crystal structure analysis, but were directly included in the final molecular formula. Further details for crystallographic data and structures are listed in Table 1. The selected bond distances and bond angles are summarized in Table S1. Crystallographic data for the structures reported in this paper have been deposited in the Cambridge Crystallographic Data Center with CCDC number of 969174 and 969175.

## 10 Results and Discussion

### Syntheses

In the process of hydrothermal synthesis, several factors can influence the formation of crystal phases, such as initial reactants, molar ratio, pH value, reaction time, temperature, etc. In this work, the pH value of the reaction system is crucial for the formation of the title complexes. Only in the pH range from 3.5 to 4.0 for **1** and the pH value of 4.5 for **2**, the suitable crystals for single crystal X-ray diffraction were obtained.

### Description of Crystal Structures

The  $[\text{CrMo}_6(\text{OH})_6\text{O}_{18}]^{3-}$  ( $\text{CrMo}_6$ ) or  $[\text{CrMo}^{\text{VI}}_5\text{Mo}^{\text{V}}(\text{OH})_6\text{O}_{18}]^{4-}$  ( $\text{CrMo}^{\text{VI}}_5\text{Mo}^{\text{V}}$ ) anion acting as inorganic building block adopts different coordination modes in complexes **1** and **2**, which possess B-type Anderson structure made up of seven edge-sharing octahedra. Six of them are  $\{\text{MoO}_6\}$  octahedra arranged hexagonally around the central  $\{\text{Cr}(\text{OH})_6\}$  octahedron. The Cr–O bond lengths are in the range of 1.951(6)–1.995(6) Å, while the O–Cr–O angles vary from 84.2(3) to 179.9(2)°. According to the coordination environments, there are four types of oxygen atoms existing in the POM unit: terminal oxygen Ot, terminal oxygen O $t'$  linked to Cu ions, double-bridging oxygen Oa and central oxygen Ob. Thus, the Mo–O bond lengths fall into four types: Mo–Ot, 1.699(7)–1.704(6) Å; Mo–O $t'$ , 1.712(6)–1.719(6) Å; Mo–Oa, 1.895(6)–1.917(6) Å; and Mo–Ob, 2.288(6)–2.306(6) Å.

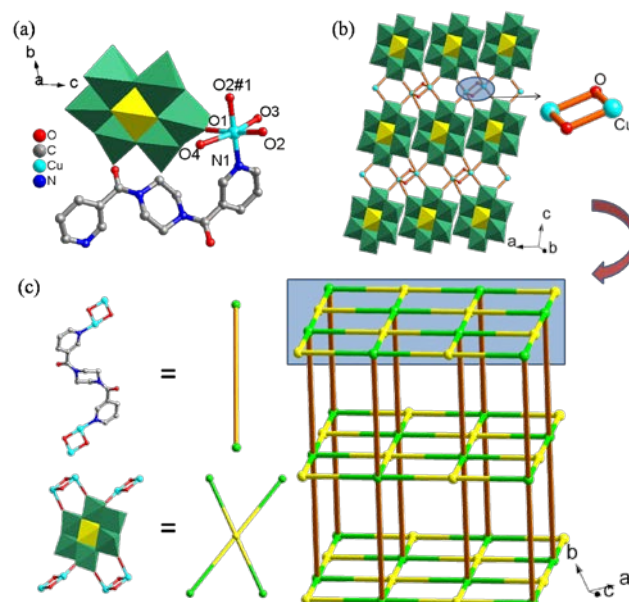
Bond valence sum calculations<sup>15</sup> show that all of the Cu ions are in the +II oxidation state in the title complexes. For **1**, six Mo atoms are in the +VI oxidation state. To balance the charge, a proton is added, then **1** is formulated as  $\text{H}[\text{Cu}_2\text{L}^1\text{Cr}(\text{OH})_6\text{Mo}_6\text{O}_{18}(\mu_2\text{-OH})_2]\cdot 4\text{H}_2\text{O}$ .<sup>16a</sup> While for **2**, five Mo atoms are in the +VI oxidation state and one Mo atom is in the +V oxidation state,<sup>16b</sup> so **2** is formulated as  $[\text{Cu}_2\text{L}^2\text{Cr}(\text{OH})_6\text{Mo}^{\text{VI}}_5\text{Mo}^{\text{V}}\text{O}_{18}(\text{H}_2\text{O})_4]\cdot 4\text{H}_2\text{O}$ .

### Crystal structure of $\text{H}[\text{Cu}_2(\mu_2\text{-OH})_2\text{L}^1[\text{CrMo}_6(\text{OH})_6\text{O}_{18}]]\cdot 4\text{H}_2\text{O}$ (**1**)

Crystal structure analysis reveals that complex **1** is a 3D POM-based MOF constructed from the Anderson-type  $\text{CrMo}_6$  anions and the bis(pyridylformyl)piperazine  $\text{L}^1$ . The asymmetric unit consists of two  $\text{Cu}^{\text{II}}$  ions, one  $\text{L}^1$  molecule, one  $\text{CrMo}_6$  polyoxoanion, two  $\mu_2$ -OH groups and four lattice water molecules. The  $\text{Cu}^{\text{II}}$  ion adopts a distorted octahedral geometry (Fig. 1a), coordinated by one N atom from one  $\text{L}^1$  ligand with Cu–N bond distance of 2.009(10) Å, three O atoms from three  $\text{CrMo}_6$  anions and two O atoms from two  $\mu_2$ -OH groups with

Cu–O bond distances of 1.936(6)–2.278(6) Å. The bond angles around the  $\text{Cu}^{\text{II}}$  ion are 83.1(3)–171.7(3)° for O–Cu–O and 91.8(3)–178.9(3)° for N–Cu–O.

As shown in Fig. 1b, two  $\mu_2$ -OH groups connect two adjacent  $\text{Cu}^{\text{II}}$  ions to form a  $\{\text{Cu}_2(\text{OH})_2\}$  dinuclear unit. Then the  $\text{CrMo}_6$  polyoxoanion cluster acts as a hexadentate inorganic ligand, providing three adjacent terminal oxygen atoms (O1, O3 and O4) and other three centrosymmetric oxygen atoms (O1#1, O3#1 and



**Fig. 1.** (a) The coordination environment of the  $\text{Cu}^{\text{II}}$  ion in **1**. The hydrogen atoms and lattice water molecules are omitted for clarity. Symmetry code:  $-x, 3-y, 1-z$ . (b) A view of the 2D Cu-POM layer in complex **1**. (c) Representation of the  $\{4^4.6^{10.8}\}\{4^4.6^2\}$  network of **1**.

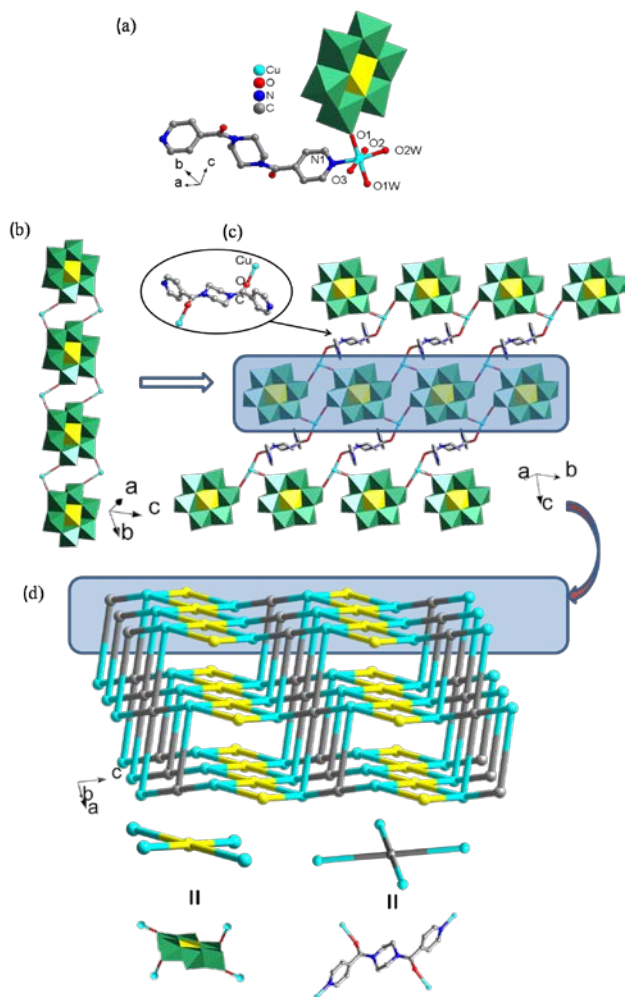
O4#1) on the same equator surface to connect six  $\text{Cu}^{\text{II}}$  ions from four adjacent  $\{\text{Cu}_2(\text{OH})_2\}$  dinuclear units (Fig. S1), which leads to the formation of the 2D Cu-POM inorganic layer in **1** (Fig. 1b). In this layer, there exists two kinds of  $\text{Cu}_2(\text{POM})_2$  loops with dimensions of ca.  $5.639 \times 3.062 \text{ \AA}^2$  and  $2.989 \times 9.175 \text{ \AA}^2$ , respectively (Fig. S2). Each  $\text{L}^1$  molecule serves as a  $\mu_2$ -bridging ligand (via ligation of pyridyl nitrogen atoms) to link two  $\text{Cu}^{\text{II}}$  ions belonging to the neighboring 2D Cu-POM inorganic layers with the  $\text{Cu}^{\text{I}}\cdots\text{Cu}^{\text{I}}$  non-bonding distance of 11.835 Å, constructing a 3D MOF (Fig. S3). It is necessary to simplify the building blocks from the 3D framework. Considering the  $\text{CrMo}_6$  polyoxoanions as the four-connected nodes, the  $\{\text{Cu}_2(\text{OH})_2\}$  dinuclear units as six-connected nodes and the  $\text{L}^1$  ligands as linear linkers, the resulting structure of **1** is a 4,6-connected net with Schläfli symbol of  $\{4^4.6^{10.8}\}\{4^4.6^2\}$  (Fig. 1c). To the best of our knowledge, complex **1** is the first 3D example of Anderson-type polyoxometalate-based MOFs constructed from bis-pyridyl-bis-amide ligands.

### Crystal structure of $[\text{Cu}_2\text{L}^2[\text{CrMo}^{\text{VI}}_5\text{Mo}^{\text{V}}(\text{OH})_6\text{O}_{18}](\text{H}_2\text{O})_4]\cdot 4\text{H}_2\text{O}$ (**2**)

Crystal structure analysis reveals that complex **2** is also a 3D Anderson-type polyoxometalate-based MOF containing 1D Cu-POM chains and the bis(pyridylformyl)piperazine  $\text{L}^2$ . However, its topological structure is obviously different from that of **1**. The symmetric unit of **2** consists of two  $\text{Cu}^{\text{II}}$  ions, one  $\text{L}^2$  ligand, one



CrMo<sup>VI</sup><sub>5</sub>Mo<sup>V</sup> anion, four coordinated water molecules and four lattice water molecules. Each Cu<sup>II</sup> ion is six-coordinated by one N atom from one L<sup>2</sup> ligand, one O atom from the carbonyl group of one L<sup>2</sup> ligand, two O atoms from two CrMo<sup>VI</sup><sub>5</sub>Mo<sup>V</sup> polyoxoanions, and two O atoms from two coordinated water molecules, showing a distorted octahedral geometry (Fig. 2a). The bond distances and angles around Cu<sup>II</sup> ion are 1.990(3) Å for Cu–N, 1.950(3)–2.385(3) Å for Cu–O and 172.55(11)° for O–Cu–O.



**Fig. 2.** (a) The coordination environment of the Cu<sup>II</sup> ion in **2**. The hydrogen atoms and lattice water molecules are omitted for clarity. (b) A view of the 1D Cu-POM chain in complex **2**. (c) Representation of the 2D network of **2**. (d) Representation of the {4<sup>2</sup>.8<sup>4</sup>} framework of **2**.

In **2**, each CrMo<sup>VI</sup><sub>5</sub>Mo<sup>V</sup> polyoxoanion acting as quadridentate inorganic ligand coordinated with four Cu<sup>II</sup> ions and connected with each other through the Cu<sup>II</sup> ions to form a 1D Cu-POM chain (Fig. 2b), in which a Cu<sub>2</sub>(POM)<sub>2</sub> loop [Cu<sub>2</sub>(CrMo<sup>VI</sup><sub>5</sub>Mo<sup>V</sup>)<sub>2</sub>] with dimension of 7.872 × 5.204 Å<sup>2</sup> can be observed (Fig. S4). It should be noted that the ligand L<sup>2</sup> adopts a μ<sub>4</sub>-bridging coordination mode [via ligation of two oxygen atoms of carbonyl groups and two nitrogen atoms of pyridine groups] coordinating with four different Cu<sup>II</sup> ions, respectively, which is different from that in complex **1**. Two carbonyl oxygen atoms of the L<sup>2</sup> ligand connect two Cu<sup>II</sup> ions from the neighboring 1D Cu-POM chains to generate a 2D inorganic-organic hybrid layer (Fig. 2c). In this

layer, there is also a [Cu<sub>2</sub>L<sup>2</sup><sub>2</sub>] metal-organic loop with dimension of 10.929 × 4.953 Å<sup>2</sup> (Fig. S5). Finally, the L<sup>2</sup> ligands through two apical pyridyl N atoms bridge two Cu<sup>II</sup> ions from the adjacent 2D layers constructing a 3D framework (Fig. S6). Topologically, the Cu<sup>II</sup> ions, the L<sup>2</sup> molecules and the CrMo<sup>VI</sup><sub>5</sub>Mo<sup>V</sup> polyoxoanions can be considered as 4-connected nodes, respectively. Thus, the structure of **2** can be described as a 4,4,4-connected net with the topology of {4<sup>2</sup>.8<sup>4</sup>} (Fig. 2d).


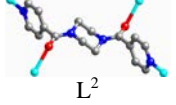


### 35 Influences of the coordination modes of the Anderson-type POM anions and the isomeric bis(pyridylformyl)piperazine ligands on the structures

Complexes **1** and **2** represent the novel examples of high dimensional Anderson-type POM-based MOFs constructed from isomeric bis(pyridylformyl)piperazine ligands. Obviously, the Anderson-type anions and the isomeric N-donor ligands show different coordination modes in complexes **1** and **2**, which exhibit important effect on the whole frameworks (Table 2). In **1**, the CrMo<sub>6</sub> anions are 6-dentate linkers coordinating with six Cu<sup>II</sup> ions to form a 2D Cu-POM inorganic layer. While in **2**, the CrMo<sup>VI</sup><sub>5</sub>Mo<sup>V</sup> anions exhibit 4-dentate linkers coordinating to four Cu<sup>II</sup> ions, forming a 1D Cu-POM inorganic chain.

On the other hand, the isomeric bis(pyridylformyl)piperazine ligands L<sup>1</sup> and L<sup>2</sup> adopt two different coordination modes in the title complexes. In complex **1**, the L<sup>1</sup> ligands with 3-substituted pyridyl ring display a μ<sub>2</sub>-bridging mode connecting two Cu<sup>II</sup> ions through Cu–N bonds, which act as the “supporter” extending the 2D inorganic grids into a 3D framework with a 4,6-connected {4<sup>4</sup>.6<sup>10</sup>.8}{4<sup>4</sup>.6<sup>2</sup>} topology. While in **2**, the L<sup>2</sup> ligands with 4-substituted pyridyl ring exhibit a μ<sub>4</sub>-bridging mode through its two pyridyl N atoms and two carbonyl O atoms, directly extending the 1D Cu-POM chain into the 3D network with a 4,4,4-connected {4<sup>2</sup>.8<sup>4</sup>} topology. Our group has reported a 2D Keggin-type POM-templated complex based on the L<sup>2</sup> ligand, in which L<sup>2</sup> ligands serve as μ<sub>2</sub>-bridging linkers.<sup>17</sup> As far as we know, the μ<sub>4</sub>-bridging coordination mode of the bis(pyridylformyl)piperazine ligands has not been found in other POM-based complexes.

As shown above, these results strongly suggest that the coordination sites of the isomeric organic ligands and the coordination modes of POM anions have essential influence on the target complexes. Therefore, an appropriate combination of the organic ligands and the different types of POMs may lead to the formation of various high dimensional structures.

Table 2. The coordination modes of the ligands (L<sup>1</sup> or L<sup>2</sup>) and the Anderson-type POM anions

	Complex <b>1</b>	Complex <b>2</b>
The ligands	 L <sup>1</sup>	 L <sup>2</sup>
The POM anions		

### IR spectra

The IR spectra of complexes **1–2** are shown in Fig. S7. The characteristic bands at 644, 824, 901  $\text{cm}^{-1}$  for **1** and 646, 885, 936  $\text{cm}^{-1}$  for **2** are attributed to the  $\nu(\text{Mo}-\text{O}_i)$ ,  $\nu(\text{Mo}-\text{O}_t)$ ,  $\nu(\text{Mo}-\text{O}_a)$  and  $\nu(\text{Mo}-\text{O}_b)$ , respectively.<sup>18</sup> The bands observed in the region of 1274, 1450, 1614  $\text{cm}^{-1}$  for **1**, for 1289, 1471, 1614  $\text{cm}^{-1}$  for **2** are due to the ligands.<sup>19</sup> The bands around 3300  $\text{cm}^{-1}$  can be attributed to the water molecules.

### Thermal stability analysis

Thermogravimetric analyses (TGA) of complexes **1** and **2** were performed in flowing  $\text{N}_2$  atmosphere with a heating rate of 10  $^\circ\text{C min}^{-1}$  from the room temperature to 800  $^\circ\text{C}$  (Fig. S8). The TGA curve of complex **1** shows two distinct weight loss steps. The first weight loss step from room temperature to 320  $^\circ\text{C}$  corresponds to the loss of water molecules and hydroxyl groups 13.32% (calcd: 13.44%). The second weight loss at 350–585  $^\circ\text{C}$  is ascribed to the loss of organic molecules 19.12% (calcd: 19.19%). For complex **2**, water molecules and hydroxyl groups are released successively from the room temperature to 350  $^\circ\text{C}$  with the weight loss of 15.46% (calcd: 15.52%).  $\text{L}^2$  ligands decompose from 380  $^\circ\text{C}$  to 642  $^\circ\text{C}$  with the weight loss of 18.06% (calcd: 18.67%). The residue can be attributed to a mixture of  $\text{CuO}$ ,  $\text{CrO}_3$  and  $\text{MoO}_3$ .<sup>20</sup>

### Powder X-ray diffraction

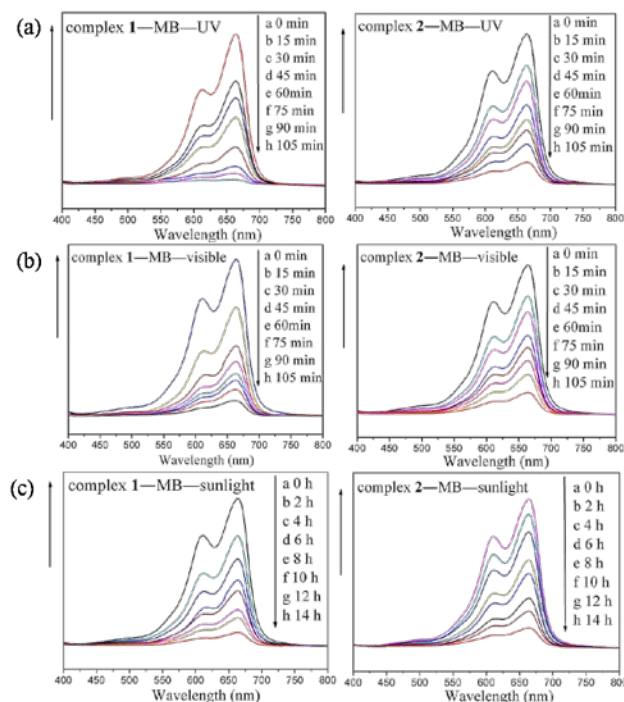
The PXRD patterns indicate that the synthesized complexes match with the simulated one except for some intensity differences, which can be owed to the different orientation of the crystals in the powder samples (Fig. S9), proving the crystalline phase purity.<sup>21</sup>

### Photocatalytic activity

It is well known that POMs often show photocatalytic activity in the degradation of some organic dyes under UV irradiation by oxidation of organic materials.<sup>22</sup> Wang's group reported two Anderson-type POM-based complexes  $\{\text{Mn}(\text{salen})_2(\text{H}_2\text{O})_2[\text{AlMo}_6(\text{OH})_6\text{O}_{18}]\} \cdot 16\text{H}_2\text{O}$  and  $\{\text{Mn}(\text{salen})_2(\text{H}_2\text{O})_2[\text{CrMo}_6(\text{OH})_6\text{O}_{18}]\} \cdot 11\text{H}_2\text{O}$  (salen =  $\text{N,N}'$ -ethylene-bis(salicylideneimine)), which showed photocatalytic activity toward the degradation of Rhodamine-B (RhB).<sup>21</sup> Accordingly, Anderson-type POM-based complexes can be taken as potential photocatalysts in the decomposition of some organic dyes. Herein, we selected an organic dye methylene blue (MB) as a model pollutant in aqueous media to evaluate the photocatalytic effectiveness of complexes **1** and **2** under UV, visible light and sunlight irradiation. Firstly, we investigated the photocatalytic performance of the title complexes for the photodegradation of MB with UV light irradiation from a 125W Hg lamp. As shown in Fig. 3(a), the absorption peak of MB decreased obviously with increasing reaction time for complexes **1** and **2** under UV irradiation. Changes in  $C/C_0$  of MB solutions versus reaction time of complexes **1** and **2** were plotted in Fig. 4(a). The calculation results show that the conversion of MB is 94.3% for **1** and 82.1% for **2**, respectively.

A few POM-based hybrids can also be used as one kind of cheap photocatalysts for the removal of organic pollutants under visible light irradiation. Recently, Wang's group reported a

Wells-Dawson-type POM-based ionic crystal  $[\text{WO}_4\{\text{Ni}(\text{en})_2(\text{H}_2\text{O})_3\}][\text{Ni}(\text{en})_3]\{\text{P}_2\text{W}_{18}\text{O}_{62}\} \cdot [\text{Ni}(\text{en})_3]\text{CO}_3 \cdot \text{H}_2\text{O}$  (en = ethanediamine), which exhibited photocatalytic activity for the degradation of MB under visible light irradiation.<sup>24</sup> However, Anderson-type POM-based hybrid complexes with excellent photocatalytic activity under visible light irradiation have not been reported yet. In this work, we also carry out the same photocatalysis experiment except that UV irradiation is replaced by visible light irradiation from a 350 W Xe lamp equipped with



**Fig. 3.** Absorption spectra of the MB solution during the decomposition reaction under UV (a), visible (b) and sunlight (c) irradiation at the presence of the title complexes.

a long-pass filter (400 nm cut off). It can be seen from Fig. 3b and Fig. 4b, the absorbance peak of MB aqueous solution decreased gradually and the decolorization of MB aqueous solution became obvious with increasing time under visible light irradiation for complexes **1** and **2**. Additionally, changes in  $C/C_0$  of MB solutions against reaction time indicate that the photocatalytic activities increase from 27.3% (without catalysts) to 88.4% for **1** and 82.2% for **2**.

Cao's group has prepared  $\text{PW}_{12}\text{O}_{40}^{3-}$ -based multilayer films on  $\text{MnCO}_3$  microspheres, which shows photocatalytic activity towards the degradation of methyl orange (MO) and RhB under sunlight irradiation.<sup>25</sup> However, the photocatalytic activity of POM-based MOFs under sunlight irradiation has not been reported yet. Herein we perform the photocatalytic tests of the title complexes towards the degradation of MB under sunlight irradiation. After being in sunlight for 14 h, the degradation efficiency is 87.4% for **1** and 83.4% for **2** (Fig. 3c and Fig. 4c). The results indicate that the Anderson-type POM-based MOFs may have important and potential application in the purification of the polluted water.

Additionally, the PXRD patterns of the title complexes after the photocatalytic reactions have been carried out, which match

with the simulated ones except for some intensity difference. (Fig. S9). The results suggest that the title complexes possess good stability as photocatalysts for the photodegradation of MB contaminant.

## Conclusions

Two 3D Anderson-type POM-based MOFs constructed from two isomeric bis(pyridylformyl)piperazine ligands and  $\text{CrMo}_6$  anions have been hydrothermally synthesized. The pH value play an important role in the assembly of both the complexes. The

coordination modes of the isomeric ligands and the Anderson-type polyoxoanions conduce to the diverse topologies of the final frameworks. The title complexes represent the first 3D examples of Anderson-type POM-based MOFs constructed from the bis-pyridyl-bis-amide ligands. In addition, the complexes **1-2** exhibit remarkable photocatalytic activities for the degradation of MB under UV, visible light and sunlight irradiation. The title complexes may be potential candidates as photocatalytic materials.

## Acknowledgements

Financial supports of this research by the National Natural Science Foundation of China (No.21171025 and 21101015), New Century Excellent Talents in University (NCET-09-0853), and Program of Innovative Research Team in University of Liaoning Province (LT2012020).

## Notes and references

- (a) C. F. Wang, J. L. Zuo, B. M. Bartlett, Y. Song, J. R. Long, X. Z. You., *J. Am. Chem. Soc.*, 2006, **128**, 7162; (b) R. Matsuda, R. Kitaura, S. Kitagawa, Y. Kubota, R. V. Belosludov, T. C. Kobayashi, H. Sakamoto, T. Chiba, M. Takata, Y. Kawazoe, Y. Mita, *Nature*, 2005, **436**, 238.; (c) F. J. Ma, S. X. Liu, C. Y. Sun, D. D. Liang, G. J. Ren, F. Wei, Y. G. Chen, Z. M. Su, *J. Am. Chem. Soc.*, 2011, **133**, 4178; (d) X. M. Zhang, Z. M. Hao, W. X. Zhang, X. M. Chen, *Angew. Chem. Int. Ed.*, 2007, **46**, 3456.
- (a) B. K. Tripuramallu, S. K. Das, *Cryst. Growth. Des.*, 2013, **13**, 2426; (b) Y. Gong, T. Wu, P. G. Jiang, J. H. Lin, Y. X. Yang, *Inorg. Chem.*, 2013, **52**, 777; (c) H. Fu, Y. G. Li, Y. Lu, W. L. Chen, Q. Wu, J. X. Meng, X. L. Wang, Z. M. Zhang, E. B. Wang, *Cryst. Growth. Des.*, 2011, **11**, 458; (d) R. G. Cao, S. X. Liu, L. H. Xie, Y. B. Pan, J. F. Cao, Y. H. Ren, L. Xu, *Inorg. Chem.*, 2007, **46**, 3541.
- (a) H. Y. An, Y. G. Li, D. R. Xiao, E. B. Wang, C. Y. Sun, *Cryst. Growth. Des.*, 2006, **6**, 1107; (b) A. Iturraspe, B. Artetxe, S. Reinoso, L. S. Felices, P. Vitoria, L. Lezama, J. M. Gutiérrez-Zorrilla, *Inorg. Chem.*, 2013, **52**, 3084.
- (a) H. Y. Liu, L. Bo, J. Yang, Y. Y. Liu, J. F. Ma, H. Wu, *Dalton Trans.*, 2011, **40**, 9782; (b) W. Q. Kan, J. Yang, Y. Y. Liu, J. F. Ma, *Inorg. Chem.*, 2012, **51**, 11266.
- (a) X. L. Wang, H. L. Hu, A. X. Tian, H. Y. Lin, J. Li, *Inorg. Chem.*, 2010, **49**, 10299; (b) X. L. Wang, C. Xu, H. Y. Lin, G. C. Liu, S. Yang, Q. Gao, A. X. Tian, *CrystEngComm*, 2012, **14**, 5836; (c) X. L. Wang, D. Zhao, A. X. Tian, J. Ying, *CrystEngComm*, 2013, **15**, 4516.
- (a) V. Shivaiah, M. Nagaraju, S. K. Das, *Inorg. Chem.* 2003, **42**, 6604; (b) L. Z. Zhang, W. Gu, Z. L. Dong, X. Liu, B. Li, *CrystEngComm*, 2008, **10**, 1318; (c) Y. Y. Yang, L. Xu, F. Y. Li, X. S. Qu, *Inorg. Chem. Commun.*, 2013, **33**, 142.
- D. Drewes, E. M. Limanski, B. Krebs, *Dalton. Trans.*, 2004, **33**, 2087.
- (a) B. K. Tripuramallu, S. K. Das, *Cryst. Growth. Des.*, 2013, **13**, 2426; (b) Y. Q. Lan, S. L. Li, X. L. Wang, K. Z. Shao, D. Y. Du, H. Y. Zang, Z. M. Su, *Inorg. Chem.*, 2008, **47**, 8179. (c) B. X. Dong, Q. Xu, *Cryst. Growth. Des.*, 2009, **9**, 2776; (d) M. G. Liu, P. P. Zhang, J. Peng, H. X. Meng, X. Wang, M. Zhu, D. D. Wang, C. L. Meng, K. Alimaje, *Cryst. Growth. Des.*, 2012, **12**, 1273.
- (a) Y. Wang, D. R. Xiao, Y. F. Qi, E. B. Wang, J. Liu, *J. Clust. Sci* 2008, **19**, 367; (b) H. Y. An, D. R. Xiao, E. B. Wang, Y. G. Li, X. L. Wang and L. Xu, *Eur. J. Inorg. Chem.* 2005, **44**, 854; (c) S. Z. Li, P. T. Ma, J. P. Wang, Y. Y. Guo, H. Z. Niu, J. W. Zhao, J. Y. Niu, *CrystEngComm*, 2010, **12**, 1718.
- V. Shivaiah, S. K. Das, *Inorg. Chem.*, 2005, **44**, 8846.
- H. Y. An, D.R. Xiao, E. B. Wang, Y. G. Li, Lin, Xu, *New J. Chem.* 2005, **29**, 667.
- Y. Hu, H. Y. An, X. Liu, J. Q. Yin, H. L. Wang, H. Zhang, L. Wang, *Dalton Trans.*, 2014, **43**, 2488.
- (a) H. W. Hou, Y. L. Song, H. Xu, Y. L. Wei, Y. T. Fan, Y. Zhu, L. K. Li, C. X. Du, *Macromolecules* 2003, **36**, 999. (b) V. Lee, Y. Sasaki, *Chem Lett*, 1984, 1274.

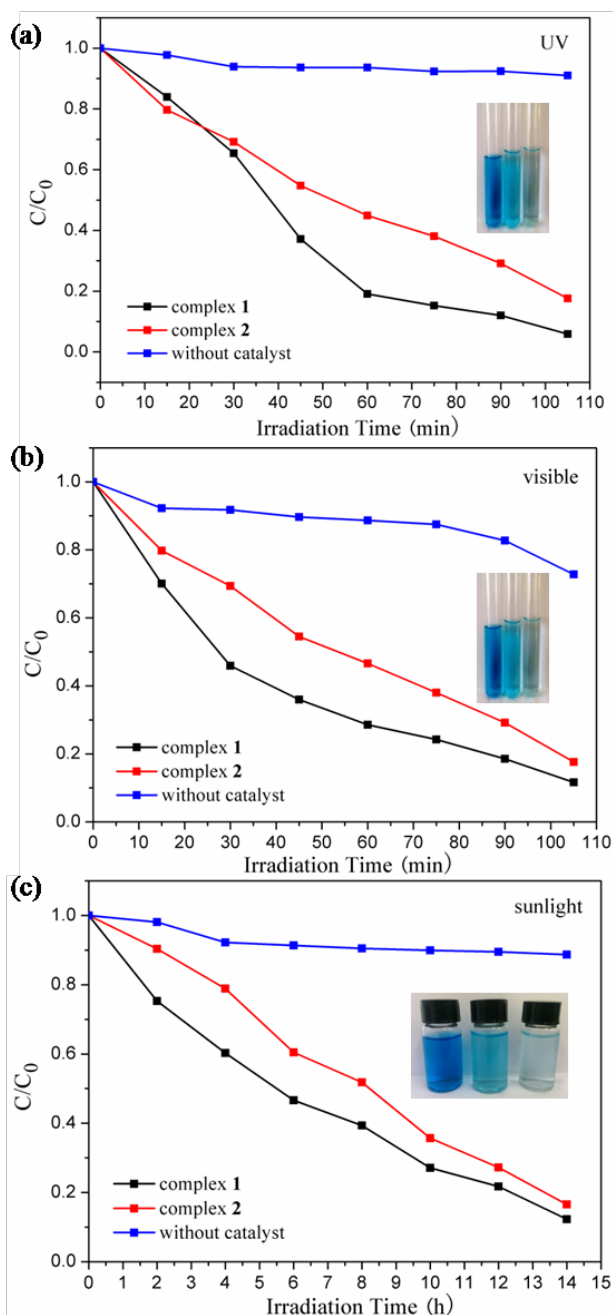


Figure 4. Photocatalytic decomposition rate of MB solution under UV (a), visible (b) and sunlight (c) irradiation with the use of complexes **1** and **2**.

- 14 G. M. Sheldrick, *Acta Crystallogr., Sect. A: Found. Crystallogr.*, 2008, **64**, 112.
- 15 I. D. Brown, D. Altermatt, *Acta Crystallogr., Sect. B*, 1985, **41**, 244.
- 16 (a) S. Z. Li, P. T. Ma, J. P. Wang, Y. Y. Guo, H. Z. Niu, J. W. Zhao, J. Y. Niu, *CrystEngComm.*, 2010, **12**, 1718; (b) L. S. Wang, P. C. Yin, J. Zhang, J. Hao, C. L. Lv, F. P. Xiao, Y. G. Wei, *Chem. Eur. J.*, 2011, **17**, 4796.
- 17 X. L. Wang, B. Mu, H. Y. Lin, G. C. Liu, A. X. Tian, J. L. Z. H. Kang, *Transition Met. Chem.*, 2010, **35**, 967.
- 18 K. Nomiya, T. Takahashi, T. Shirai, M. Miwa, *Polyhedron*, 1987, **6**, 213.
- 19 K. Uehara, T. Oishi, T. Hirose, N. Mizuno, *Inorg. Chem.*, 2013, **52**, 11200.
- 20 (a) S. W. Zhang, Y. X. Li, Y. Liu, R. G. Cao, C. Y. Sun, H. M. Ji, S. X. Liu, *J. Mol. Struct.*, 2009, **920**, 284; (b) D. Dutta, A. D. Jana, M. Debnath, A. Bhaumik, J. Marek, *Dalton Trans.*, 2010, **39**, 11551.
- 21 A. X. Tian, J. Ying, J. Peng, J. Q. Sha, H. J. Pang, P. P. Zhang, Y. Chen, M. Zhu, Z. M. Su, *Cryst. Growth. Des.*, 2008, **8**, 3717.
- 22 (a) J. Tucher, Y. L. Wu, L. C. Nye, I. Ivanovic-Burmazovic, M. M. Khusniyarov, C. Sterb, *Dalton Trans.*, 2012, **41**, 9938; (b) A. Dolbecq, P. Mialane, B. Keita, L. Nadjo, *J. Mater. Chem.*, 2012, **22**, 24509; (c) P. P. Zhang, J. Peng, H. J. Pang, J. Q. Sha, M. Zhu, D. D. Wang, M. G. Liu, Z. M. Su, *Cryst. Growth. Des.*, 2011, **11**, 2736.
- 23 Q. Wu, W. L. Chen, D. Liu, C. Liang, Y. G. Li, S. W. Lin, E. B. Wang, *Dalton Trans.*, 2011, **40**, 56.
- 24 Z. J. Liu, S. Yao, Z. M. Zhang, E. B. Wang, *RSC Adv*, 2013, **3**, 20829.
- 25 S. Y. Gao, R. Cao, J. Lv, G. L. Li, Y. F. Li, H. X. Yang, *J. Mater. Chem.*, 2009, **19**, 4157.



# Assembly and photocatalysis of two novel 3D Anderson-type polyoxometalate-based metal-organic frameworks constructed from isomeric bis(pyridylformyl)piperazine ligands

Xiuli Wang,\* Zhihan Chang, Hongyan Lin, Aixiang Tian, Guocheng Liu, Juwen Zhang

Two 3D Anderson-type polyoxometalate-based metal-organic frameworks constructed from two isomeric bis(pyridylformyl)piperazine ligands have been hydrothermally synthesized and characterized. The isomeric ligands and Anderson-type polyanions show different coordination modes in complexes **1–2**, which play key roles in the construction of the final frameworks. The photocatalytic properties of the title complexes have been investigated systematically.

